北海道大学工学部研究報告
第 140 号（昭和 63 年）

Bulletin of the Faculty of Engineering,
Hokkaido University. No. 140 (1988)

Surface Area and Outgassing Behaviors of Various Isotropic Graphites as Nuclear Fusion Material

Y. HIROHATA, S. FUKUDA, T. HINO and T. YAMASHINA

(Recieved December 26, 1987)

Department of Nuclear Engineering, Hokkaido University, Sapporo Japan

Abstract

Surface areas and outgassing behaviors of various isotropic graphites were investigated by using the physisorption of xenon at 77 K and a thermal desorption spectroscopy (TDS), respectively. The specific surface areas ranged from 0.4 to 1.34 m^2/g and hand a tendency to increase with the apparent density. The main gases desorbed from graphites were H_2, H_2O, CH_4, CO, CO_2, and hydrocarbons. The total amount of desorbed gases increased with the specific surface area. The purification after graphitization was effective for the reduction of the outgassing.

Introduction

Graphite is regarded as one of the candidate materials for the first wall elements of nuclear fusion devices because of the adequate properties- such as low atomic number, high melting point, thermal shock resistance and thermal conductivity.[1)-2)] On the other hand, graphite is known as a highly porous material.[3)-4)] Therefore, there is the question concerning the outgassings due to heat load from plasma and the gas uptake during the maintenance of a vacuum chamber, in a case where the bulk graphite tiles are installed in the interior of the vacuum chamber. The purpose of this work is to investigate the outgassing levels and surface areas of various isotropic graphites and find a correlation between them.

Experimental

Isotropic graphite samples with the apparent densities (d) ranging from 1.6 to 2.0 g/cm^3 were supplied by seven Japanese manufactures. Table 1 presents the physical properties of the samples. Most of them were manufactured by the isotropic rubber press method (Isostatic pressing) and some of them by mold pressing.

Their surface areas were measured by the BET method.[5)-6)] In order to obtain adsorption isotherms, physical adsorption of xenon at liquid nitrogen temperature was utilized. The details of the apparatus was already reported.[7)-8)] The procedure of the measurement is as follows. A graphite sheet with a thickness of 0.5 mm was cut into the size of $5\times5\times0.5$ mm. All samples have roughly a constant geometrical surface area. Their weights vary from 24 to 28 mg. They were degassed at 300°C for 20 hr under a pressure of about 1×10^{-5} Pa prior to the measurement. After the baking of the system and outgassing of the samples, the sample cell made of quartz glass was immersed in liquid nitrogen. Because a specimen

Table. 1 Physical constants of graphite materials

Manufactures / Sample name	A			B			C		D		E		F				G	
	A-1	A-2	A-3	B-1	B-2	B-3	C-1	C-2	D-1	D-2	E-1	E-2	F-1	F-2	F-3	F-4	G-1	G-2
Apparent density (g/cm^3)	1.90	1.82	1.77	1.91	1.78	1.75	1.88	1.60	1.95	1.80	1.98	1.82	1.82	1.80	1.77	2.0	1.75	1.65
Anisotropy ratio	1.02	1.05	1.05	1.03	1.02	1.10			1.6	1.05	1.2	1.05	1.07	1.08	1.07	4.0	1.04	2.3
Ash content (ppm)	2	2	2	20	20	10	1500	1000	5	5	10	10	10	10	10	10	500	500
Grain size(μm)	5	10	14	1	10	40			40	60	5	20	5	10-15	15	10-15	12	7
Pore size (μm)	0.4	1.1	3	0.5	1	2			0.5	4	0.5	5	2	1.4	3	0.7	2.5	1.5
Porosity (%)	11/12	12/14	14/18	9	15	13			8	13	1.0	12	16/18	16/18	16/18	7/8		
Forming	ISO	ISO	ISO	ISO	ISO	ISO			MOLD	ISO	MOLD	ISO	ISO	ISO	ISO	MOLD	ISO	MOLD
Treatment	Halogen gas Baking in Vac. (2000℃)			Halogen gas (2000℃)														

placed in ultra high vacuum was not easily cooled down to 77 K,[9] helium gas with a pressure of 10 Pa was introduced into the cell as a coolant. After the temperature of the sample became 77 K, the helium gas was pumped out and then adsorbate gas, i. e. xenon was introduced. Since the adsorption reaction is limited by the diffusion of xenon molecules through pores, it took from 0.5 to a 2 hrs to obtain one adsorption point. The BET equation derived from a adsorption isotherm give the surface area (S). Specific surface area (S/W ; m^2/g) and surface roughness factor (S/S_G) are defined as a ratio of measured surface area to sample weight and to geometrical surface area, respectively. The cross sectional area of a xenon molecule was taken as 0.25 nm^2.[10]

The outgassing behavior of the various isotropic graphites was studied by using a thermal desorption spectroscopy (TDS) device, whose schematic diagram is shown in Fig. 1.[11] The TDS apparatus consists of a main vacuum chamber and a sample preparation chamber. The ultimate pressure of the main chamber evacuated by a turbomolecular pump is routinely maintained about 2×10^{-6} Pa. The sample preparation chamber sealed with a gate valve against the main chamber is evacuated by a diffusion pump and enables us to exchange samples without exposing the main chamber to the atmosphere. Two or three pieces of a graphite samples of size of $5\times5\times0.5$ mm and with a total weight between 70 and 90 mg were placed in a container made of Ta. After the pressure of the preparation chamber reached about 1×10^{-4} Pa, the gate valve was opened and the container was introduced into the main chamber. An infrared light furnace with a power of 1.2 KW heated up the container from room temperature to 1300 K with a heating rate of 10 K/min. The temperature was monitored with an alomerl-cromel thermocouple spot-welded to the container. Thermally desorbed gases

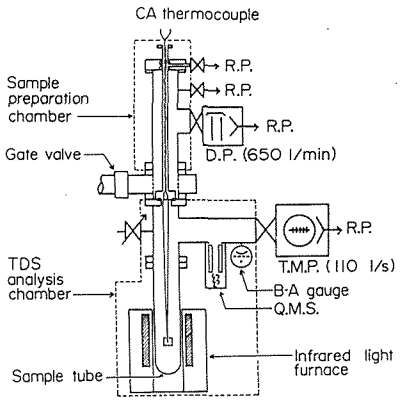

Fig. 1 The Schematic diagram of thermal desorption spectroscopy (TDS)

were analyzed by a quadrupole mass spectrometer (QMS), which scans the mass range from m/e=2 to m/e=45 with a 2 minute period. TDS spectra were obtained by substracting the background of Ta container from a obtained desorption curve. The amounts of desorbed gases were estimated, using the sensitivity factor (R_i) of QMS and the pumping speed (S_i) which were already measured for H_2, D_2, He, CH_4, N_2 and Ar. R_i and S_i of other gas species, such as CO and hydrocarbons were calculated from the ionization cross section and mass number of each gases. Reproducibility of the amount of the desorbed gases were within 20% or thereabouts.

Results and Discussion

Typical adsorption isotherms for graphite with different densities are shown in fig. 2. Here, Pe, Ps and V are the equilibrium pressure, the saturation vapor pressure of Xe, and the amount adsorbed at Pe, respectively to be saturated. The adsorption curves of each sample show a tendency to saturate around the relative pressure of 0.2.[12)-14)] Specific surface areas of these samples (A-1, 2, 3) with densities of 1.9, 1.82 and 1.77 g/cm^3 were estimated as 1.34, 0.8 and 0.7 m^2/g. Reproducibility of the surface areas were within about 10%. Figure 3 shows the relation between the apparent densities and measured specific surface areas. The specific surface areas ranged from 0.4 to 1.34 m^2/g. These values are much lower than those of graphite powders and activated carbons with the pore distribution and grain size greatly different from those of the isotropic graphite.[15)-20)] In addition, the obtained values are still larger than the surface area calculated based on the average pore diameter and the open pore volume with the assumption that the shape of pore is cylindrical. The solid line, the dotted line and the dashed line in fig. 3 correspond to the values of samples supplied by manufacturer A, B and C, respectively. At for the samples by the same manufactures, the specific surface area becomes higher as the apparent density increases. This relation may be due to that a graphite with higher apparent density is made by filling the pores of a lower density graphite with pitches, and then has larger number of pores with a smaller diameter which contribute to the increase of the surface area. Another possible reason for the above relationship is that the process to make a high density isotropic graphite inevitably includes the extremely fine pulverizing of raw material.[21)] This powdering also seems to increase the surface area, even after graphitization. The relation

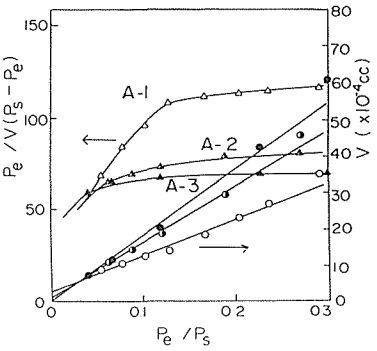

Fig. 2 Typical adsorption isotherms and BET polts of isotropic graphites

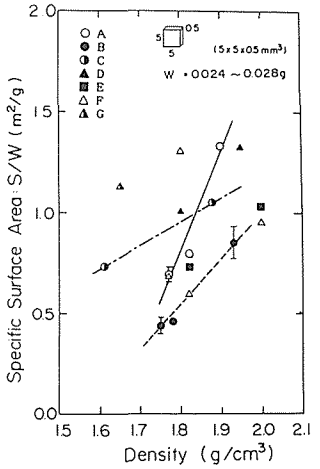

Fig. 3 The relation between the apparent density and specific surface areas

of the surface roughness factor with the apparent density was similar to that of the specific surface area. The scattering in values in fig. 3 is probably due to the difference in pore size distributions and pore volumes, which depend not only on the manufacturing process but also on the raw materials such as pitches and cokes.[21]

The effects of the thickness of the samples on the specific surface area is shown in fig. 4. Samples with different thicknesses from 0.1 mm to 1.0 mm were used for the experiments. Specific surface areas decreased with the increase of the thickness up to 0.5 mm. Above 0.5 mm, the specific surface areas were almost constant. This tendency can be interpreted as a reflection of the internal pore structure. The pores can be classified into two groups, i. e. open pores and closed pores.[16] The total length of all open pores becomes longer in proportion to the volume or the weight of a sample and contributes to the internal surface area. Here, we define A (m^2/cm^3) as the ratio of the internal surface area to volume. On the other hand, closed pores which are opened near the surface region contribute to the increase of external surface area, which should be proportional to the geometrical surface area. Here, we define B (m^2/cm^2) as the ratio of the external surface area to the geometrical surface area. The measured surface area should be the sum of both contributions. Therefore, for the case where a sample has the size of $0.5\times0.5\times t$ cm, the surface area (S) and specific surface area (S/W) are expressed by the following equations;

$$S=0.25\,At+2B\,(0.25+t) \qquad (1)$$

$$S/W=(2B/d)\,(1/t)+(A+8B)/d \qquad (2)$$

where d and t are the density and thickness, respectively.

A and B can be determined experimentally by plotting S/W versus the reciprocal of thickness, according to Eq.(2). Solid lines in fig. 4 calculated from Eq.(2) agree well with the experimental values. As the thickness increases, the surface area depends mainly on A, while B is the

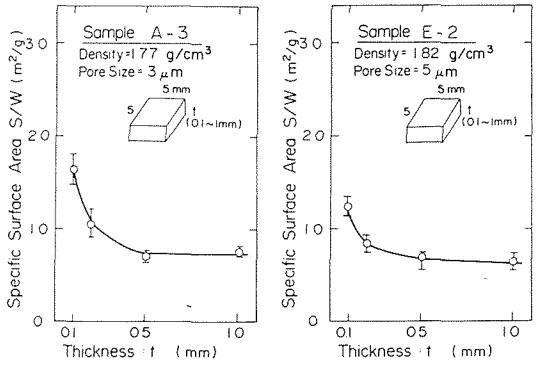

Fig. 4 The effects of the sample thickness on the specific surface areas

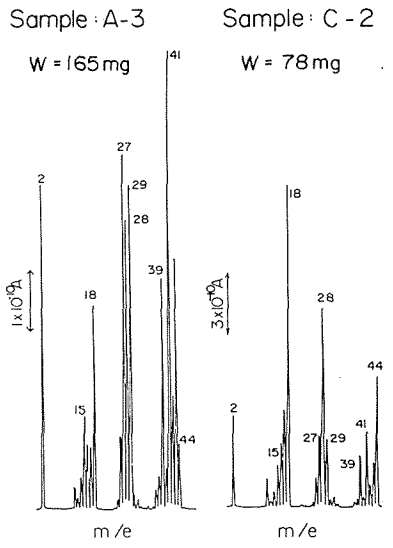

Fig. 5 Typical mass spectra of gases released at 500°C from graphite
A-3 sample; purified with high temperature halogen gas and baked in vacuum
(sample weight=165 mg)
C-2 Sample; untreated after graphitization
(sample weight=78 mg)

dominant factor when a sample thickness is less than 0.2 mm. The introduction of two factors, A and B, makes it possible to explain the results in fig. 4, satisfactorily.

Figure 5 shows the mass spectra of gases released at 500 °C from two different species of isotropic graphite. The sample, C-2, had no further treatment after graphitization, and the other one, A-3, had been purified by high temperature halogen gas to reduce the ash content down to 2 ppm and subsequently outgassed in vacuum at high temperature. Desorbed gases were mainly H_2, H_2O, CH_4, CO, CO_2 and higher hydrocarbons.[22)-23)] Cracking patterns of hydrocarbons also appeared in the mass range from 26 to 30 and from 37 to 44. Signal intensities, proportional to the outgassing rate of each gas from C-2 were obviously than from A-3. This means that the purification by halogen gas and the following annealing in vacuum were very effective to reduce the subsequent outgassing. It should be noted that the relative intensities of C_2 and C_3 hydrocarbons in the mass spectrum of A-3 (m/e=27, 29, 39, 41, 43) are higher than that of C-2. Thermal desorption spectra of m/e=28 and 44 from B-1 and C-2 with specific surface areas of 0.84 and 0.74 m^2/g are compared in fig. 6. B-1 was purified in halogen gas but not outgassed in vacuum after graphitization. Peak temperatures of m/e=28 (CO^+, $C_2H_4^+$) and 44 (CO_2^+, $C_3H_8^+$) from both samples coincide and do not depend on the treatments. If it is assumed that only CO and CO_2 is estimated 2.8×10^{17} molec./g, which is three times larger than B-1, and CO_2 is 3.2×10^{17} molec./g, which is one order larger than B-1.

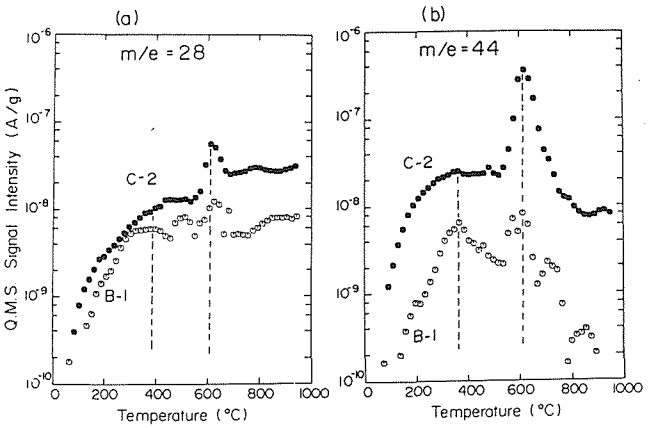

Fig. 6 Thermal desorption spectra of m/e=28 and 44
B-1 sample ; purified with high temperature halogen gas
(density = 1.91 g/cm³, S/W = 0.84 m²/g)
C-1 sample ; untreated after graphitization
(density = 1.60 g/cm³, S/W = 0.74 m²/g)

Thermal desorption spectra of H_2 and H_2O from B-1, -2, -3 are shown in fig. 7. As the apparent densities increases, signal intensity of QMA increases. The peak temperatures in the H_2 desorption

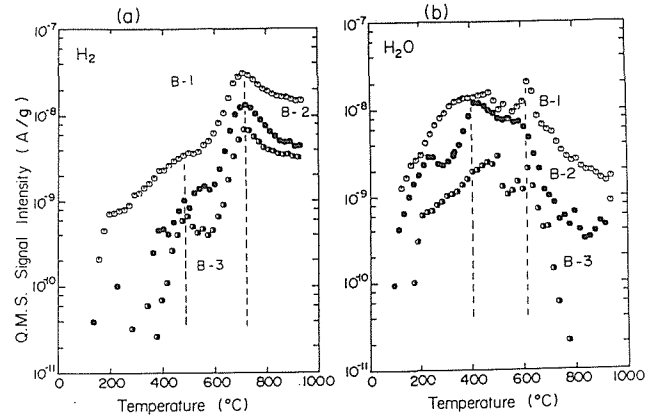

Fig. 7 Thermal desorption spectra of H_2 and H_2O
B-1 sample ; density = 1.91 g/cm³, S/W = 0.84 m²/g
B-2 sample ; density = 1.78 g/cm³, S/W = 0.54 m²/g
B-3 sample ; density = 1.75 g/cm³, S/W = 0.44 m²/g

spectra are in a good agreement. This indicates that the mechanism of H_2 desorption is identical in each case. But the peak at low temperature of H_2O desorption spectra curve slightly shifted from each other. This shift might be due to the difference in the surface morphology and the pore structure of the samples, since at low temperature H_2O is known to have a very long mean adsorption time, which greatly affects the desorption behavior especially in the case where the re-adsorption can not be neglected. The increase of the total pressure which is the sum of the partial pressures of each gas species was observed at 400°C, 600°C and 800°C in the range up to 1000°C.

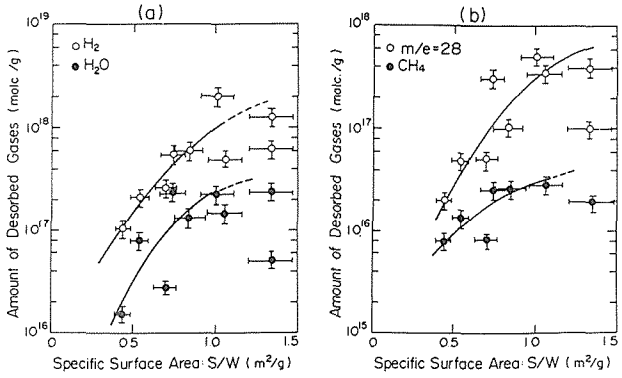

Fig. 8 The relation between the amount of desorbed gases and specific surface areas
(a) H_2 and H_2O (b) CH_4 and CO (m/e=28)

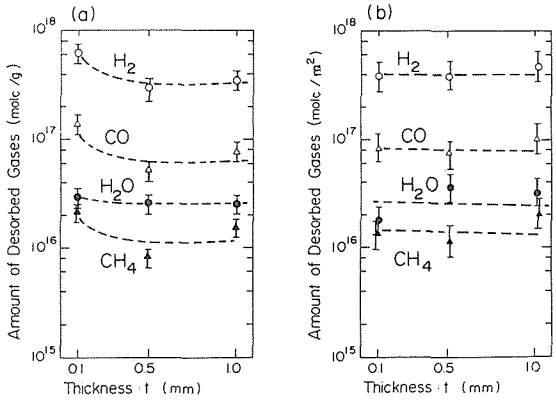

Fig. 9 Effect of sample thickness on the amount of desorbed gases
(a) The amount of desorbed gases versus the sample weight
(b) The amount of desorbed gases versus the measured surface area

Figure 8 shows the relation between the amount of desorbed gases and specific surface area. Since all samples analyzed here were exposed to the atmosphere for a long period of more than several months time, the sorption of gases into the sample presumably reached a saturation. It was found that the amount of H_2, H_2O, CH_4 and CO increased with the specific surface area. This result suggests that the amount of gas uptake directly corresponds to the specific surface area. Figure 9 shows the relation between amount of desorbed gases and the sample thickness. The same relation as seen for specific surface area against sample thickness was obtained. Therefore the amountt of desorbed gases normalized with the measured surface area becomes almost constant within the error shown fig. 9-b. In case of A-3, the amounts of adsorbed H_2 and CO are estimated to be about 10^{17} molec./m^2, and H_2O and CH_4 are about 10^{16} molec./m^2. These values correspond to the surface coverage ratio from 0.001 to 0.01.

Conclusion

Surface areas and outgassing behaviors of various isotropic graphites were investigated.

The specific area ranged from 0.4 to 1.3 m^2/g and increased with the apparent density. But a strict linearity was not found probably because of the difference in the manufacturing processes and raw materials.

H_2, H_2O, CH_4, CO and higher hydrocarbons were the main desorbed gases. The amount of desorbed gases increased with the specific surface area. The purification by high temperature halogen gas treatment and the subsequent vacuum annealing were effective to reduce the outgassings even after exposure to the air for a lengthy period of time.

These results lead us to the conclusion that isotropic graphite with low specific surface areas, which is purified by halogen gas at high temperature and annealed in vacuum, is most suitable to apply for fusion devices in order to reduce the gas release.

Acknowledgment

The authors with to thank seven Japanese manufactures, Ibiden Co., Nippon Steel Chemical Co., Tokai Carbon Co., Toyo Carbon Co., Toyo Tanso Co., Hitachi Chemical Co. and Nippon Carbon Co. for their contribution of various isotropic graphites.

This work was done under the Special Research Project on Nuclear Fusion supported by a Grant -in -Aid for fusion research.

References

1) G. M. McCraken and F. E. Stott; Nuclear Fusion 19 (1979) 889
2) M. Ulrickeson, J. L. Cecchi, B. L. Doyle, H. F. Dylla, S. S. Medley, D. K. Owems and P. W. Trester; J. Nucl. Mater. 133/134 (1985) 253
3) K. Nakayama, S. Fukuda, T. Hino and T. Yamashina; J. Nucl. Mater. 145/147 (1987) 301
4) R. A. Strehlow; J. Vac. Sci. Technol. A4 (1986) 1183
5) S. Brunauer, P. H. Emett and E. Teller; J. Ame. Chem. Soc. 60 (1938) 308
6) D. H. Young and A. D. Crowell; "The Physical adsorption of gases" Butter Worth (1962)
7) K. Watanabe and T. Yamashina; J. Catalysis 17 (1970) 272
8) K. Watanabe and T. Yamashina; Vacuum 22 (1972) 183
9) S. Chu Liang; J. Phys. Chem. 57 (1953) 84
10) W. A. Cannon; Nature197 (1963) 1000
11) T. Satake, M. Mohri, T. Yamashina, N. Noda, K. Toi, S. Tanahashi, J. Fujita; J. Nucl. Mater. 128/129 (1984) 190
12) M. H. Polley, W. D. Schaffer and W. R. Smith; J. Phys. Chem. 57 (1953) 469
13) J. H. Singleton and G. D. Halsey; J. Phys. Chem. 58 (1954) 1011
14) J. W. Ramsey; Fuel 44 (1965) 277
15) S. Hirano, M. Ozawa and S. Naka; J. Mater. Sci. 16 (1981) 1989
16) B. T. Kelly; "Physics of Graphite" Applied Science Publishers (1981)
17) R. A. Starehlow; J. Vac. Sci. Technol. A4 (1986) 1183
18) R. B. Anderson; Fuel 44 (1965) 443, 41 (1962) 559
19) K. A. Kini; Fuel 42 (1963) 103, 43 (1964) 173
20) N. Setaka, S. Matsumoto, H. Kanda and Y. Sato; Carbon 17 (1979) 303
21) Ed. Soc of Japan Tanso; "Carbon Materials" (1985)
22) A. E. Pontau and D. H. Morse; J. Nucl. Mater. 143A (1986) 124
23) A. E. Pontau, R. A. Causey and J. Bohdansky; J. Nucl. Mater. 145/147 (1987) 775